David Taylor Research Center

Bethesda, MD 20084–5000

Response of Regularly Ribbed Fluid Loaded Panels

by
G. Maidanik
J.Dickey

DTIC
S ELECTE D
DEC 20 1990
B

MAJOR DTRC TECHNICAL COMPONENTS

CODE 011   DIRECTOR OF TECHNOLOGY, PLANS AND ASSESSMENT

     12   SHIP SYSTEMS INTEGRATION DEPARTMENT

     14   SHIP ELECTROMAGNETIC SIGNATURES DEPARTMENT

     15   SHIP HYDROMECHANICS DEPARTMENT

     16   AVIATION DEPARTMENT

     17   SHIP STRUCTURES AND PROTECTION DEPARTMENT

     18   COMPUTATION, MATHEMATICS & LOGISTICS DEPARTMENT

     19   SHIP ACOUSTICS DEPARTMENT

     27   PROPULSION AND AUXILIARY SYSTEMS DEPARTMENT

     28   SHIP MATERIALS ENGINEERING DEPARTMENT

DTRC ISSUES THREE TYPES OF REPORTS:

1. **DTRC reports, a formal series,** contain information of permanent technical value. They carry a consecutive numerical identification regardless of their classification or the originating department.

2. **Departmental reports, a semiformal series,** contain information of a preliminary, temporary, or proprietary nature or of limited interest or significance. They carry a departmental alphanumerical identification.

3. **Technical memoranda, an informal series,** contain technical documentation of limited use and interest. They are primarily working papers intended for internal use. They carry an identifying number which indicates their type and the numerical code of the originating department. Any distribution outside DTRC must be approved by the head of the originating department on a case-by-case basis.

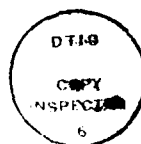# David Taylor Research Center

Bethesda, MD 20084–5000

Response of Regularly Ribbed Fluid Loaded Panels

by
G. Maidanik
J. Dickey

CONTENTS

DTIC
COPY
INSPECTED
6

Accession For

NTIS GRA&I	☑
DTIC TAB	☐
Unannounced	☐
Justification	

By

Distribution/

Availability Codes

| Dist | Avail and/or Special |
| A-1 | |

ABSTRACT

This paper presents computer estimations of the response of models of mechanically driven regularly ribbed fluid loaded panels. The estimates are presented in terms of the spectral distribution of the acceleration of the panel and the spectral distribution of the pressure in the fluid. The ribs are defined in terms of line and line moment impedances; these may be mass, resistance, and/or stiffness controlled, and of various values and combinations. Typical estimations of the spectral distribution of the magnitudes of the acceleration are displayed as functions of the normalized wavenumber that lies in the plane of the panel and normal to the ribs and the normalized frequency. The magnitudes of the acceleration vanish at the sonic loci when fluid loading is included. A sonic gorge, with a nadir at the sonic loci, characterizes the acceleration of the fluid loaded panel, whether unribbed or ribbed. If the magnitudes of the line impedances (and, when appropriate, also the line moment impedances) of the ribs are not unusually high, the magnitudes of the acceleration and their patterns elsewhere in the spectral domain remain substantially similar to those obtained in the absence of fluid loading. The dissimilarities are readily accounted for by straightforward arguments relating to the increase in the surface mass and the radiation damping that manifest fluid loading on panels. The corresponding magnitudes of the pressure on the surface of the panel do not vanish at the sonic loci as do the magnitudes of the acceleration. Rather, a moderate sonic peak appears at the sonic loci and a sonic ridge replaces the sonic gorge. The loss of subsonic components in the pressure on a plane, as the plane is removed from the surface of the panel, is clearly displayed.

ADMINISTRATIVE INFORMATION

1

INTRODUCTION

A recent paper formulated the acoustic behavior of ribbed panels immersed in uniform environments and presents computer estimations that examined and illustrated some aspects of the formalism [1]. The response of a ribbed panel to a specific external drive is presented in terms of the spectral distribution of the velocity (acceleration or displacement) on the panel and the pressure on a plane at or above the panel. An external drive is a drive which is independent of the response of the dynamic system that it excites. In this paper, the specific external drive is a line drive that it is oriented parallel to the ribs. The estimations that are computed can be employed, for example, in the design of spectral (wavevector-frequency) filters destined to measure, in real situations, similar responses on similar dynamic systems. In a companion paper such considerations were conducted on panels that were membranes and the environmental loadings were ignored [2]. A major emphasis in Reference 2 was placed on the comparison between panels to which a finite and an infinite number of ribs were attached. (It would help the reader to be familiar with the material discussed in References 1 and 2.) This paper considers a more elaborate model of a ribbed panel which may be plate-like, and fluid loading is included. However, only regularly ribbed panels are considered; i.e., panels to which an infinite number of identical and regularly spaced ribs are attached. For a regularly ribbed panel, one derives the spectral distribution of the velocity $V(k, \omega_2)$ in terms of the impulse response function $G(k \mid k', \omega_2)$ and the external drive $P_e(k', \omega_2)$ both expressed in the spectral domain; namely,

$$V(k, \omega_2) = \int G(k \mid k', \omega_2) \, dk' \, P_e(k', \omega_2); \quad A(k, \omega_2) = i\omega V(k, \omega_2);$$

$$D(k, \omega_2) = (i\omega)^{-1} V(k, \omega_2), \tag{1}$$

$$G(k \mid k', \omega_2) = G_\infty(k, \omega_2) \{ \delta(k-k') - S_s(k \mid k', \omega_2) \} , \tag{2}$$

$$S_s (k \mid k', \omega_2) = [1 + \sum_j \widetilde{H}_\infty (k + \kappa_j, \omega_2)]^{-1} \widetilde{H}_\infty(k', \omega_2) \begin{cases} \sum_n \delta (k + \kappa_n - k') \\ (\kappa_1)^{-1} \sum_n \exp [ix_n (k - k')] \end{cases} . \quad (3)$$

[cf. Eqs. (8), (9), and (11b) of Reference 2.] In Eq. (1) the spectral distributions of the velocity V (k, ω_2), the acceleration A (k, ω_2), and the displacement D (k, ω_2) on the panel are related. The relationship is simple so that using one form of the response of the panel rather than another is a matter of convenience. In Eqs. (2) and (3), $G_\infty(k, \omega_2)$ is the surface admittance of the unribbed panel, x_n is the position in the x-domain of the (n)th rib, κ_j is the separation wavenumber, $\kappa_j = j\kappa_1$, $\kappa_1 = (2\pi/b)$, where b is the separation between two adjacent ribs, and $\widetilde{H}_\infty$ (k, ω_2) is the product of the equivalent surface impedance of a rib and the surface admittance of the unribbed panel. (When the ribs are absent, b serves merely as a linear spatial scale factor.) The explicit expression for $\widetilde{H}_\infty$ (k, ω_2) is

$$\widetilde{H}_\infty (k, \omega_2) = (\kappa_1/2\pi) [Z (\omega_2) - ik Z_M(\omega_2)] G_\infty (k\omega_2) \quad , \quad (4)$$

where $Z (\omega_2)$ and $Z_M(\omega_2)$ are the line impedance and the line moment impedance of a typical rib. (The line moment impedance $Z_M(\omega_2)$ is a viable quantity only when the panel can support a moment response; e.g., a plate responding in flexure. Otherwise, $Z_M(\omega_2)$ needs to be set equal to zero [2].) The spectral vector $\omega_2 = \{k_y, \omega\}$ designates the Fourier conjugate of y and t; y is the spatial variable that lies along the ribs in the plane of the panel and t is the temporal variable; see Fig. 1. The dependence of a quantity on the spectral vector variable ω_2 is suppressed at times as a matter of abbreviation; e.g., $G_\infty(k, \omega_2) \equiv G_\infty(k)$. Note that $S_s (k \mid k', \omega_2)$, stated in Eq. (3), is aliased in the wavenumber k with respect to the harmonics of the separation wavenumber κ_1. This aliasing is transmitted also to the drive in lieu of the ribs; the aliasing in the latter quantity was discussed briefly [2]. The aliasing in k with respect to the harmonics of κ_1 may be stated in the

3

form $S_s (k \mid k') \equiv S_s(k + \kappa_j \mid k')$. [cf. Eq. (13) of Reference 2.] The external drive employed in this paper is of the form

$$P_e (k', \omega_2) = P_{ea} (\omega_2) \exp (ik'x_a) \quad . \tag{5a}$$

This form of the external line drive qualifies as follows: The external line drive $p_e(x, \omega_2)$ is assumed to be applied centrally at x_a so that about this position its description is $p_{ee}(x - x_a, \omega_2)$. It follows that $p_e(x, \omega_2) \equiv p_{ee}(x - x_a, \omega_2)$. Then, by a Fourier transformation, one obtains $P_e(k, \omega_2) = P_{ee}(k, \omega_2) \exp (ikx_a)$, where typically one defines $P_{ee}(k) = (2\pi)^{-1/2} \int dx \, p_{ee}(x) \exp (ikx)$. Furthermore, if the external line drive is localized at x_a so that

$$p_{ee}(x - x_a, \omega_2) \equiv (2\pi)^{1/2} P_{ea}(\omega_2) \delta(x - x_a) \quad , \tag{5b}$$

then $P_{ee}(k, \omega_2) = P_{ea}(\omega_2)$ and Eq. (5a) is explained. From Eqs. (1) through (3) and (5) one obtains

$$V(k, \omega_2) = V_\infty(k, \omega_2) \left\{ 1 - \right.$$
$$\left. [1 + \sum_j \tilde{H}_\infty(k + \kappa_j, \omega_2)]^{-1} \sum_n \tilde{H}_\infty(k + \kappa_n, \omega_2) \exp(ix_a\kappa_n) \right\} \quad , \tag{6}$$

where

$$V_\infty(k, \omega_2) = G_\infty(k, \omega_2) P_{ea}(\omega_2) \exp(ix_ak) \quad . \tag{7}$$

PARAMETRIC DEFINITION OF THE FLUID, THE PANEL, AND THE RIBS

To facilitate the estimation of $V(k, \omega_2)$ [$A (k, \omega_2)$ or $D (k, \omega_2)$] as stated in Eqs. (1) and (6), it remains to express more explicitly the quantities and parameters that are involved in this equation. The surface admittance of the panel is expressed in the form

4

$$G_\infty(k, \omega_2) = [Z_p(k, \omega_2) + Z_\ell(k, \omega_2)]^{-1} \; ; \quad Z_\ell(k, \omega_2) = Z_{t\ell}(k, \omega_2) + Z_{b\ell}(k, \omega_2), \tag{8}$$

where $Z_\ell(k, \omega_2)$ is the loading on the panel by the uniform environment, $Z_{t\ell}(k, \omega_2)$ is this loading on one (top) surface and $Z_{b\ell}(k, \omega_2)$ is this loading on the other (bottom) surface of the panel, and $Z_p(k, \omega_2)$ is the mechanical surface impedance of the panel [1].

In this paper the environmental loading is limited to that of a semi-infinite fluid occupying the space above the panel as shown in Fig. 1. The fluid loading on the panel may then be expressed in the form [1, 2]

$$Z_\ell(k, \omega_2) = Z_{t\ell}(k, \omega_2) = \rho\omega/k_3 = \rho c (k_3 c/\omega)^{-1} \quad , \tag{9}$$

where ρ is the density and c is the speed of sound in the fluid and

$$(k_3 c/\omega) = [1 - \mathrm{k}^2]^{1/2} U [1 - \mathrm{k}^2] - i [\mathrm{k}^2 - 1]^{1/2} U [\mathrm{k}^2 - 1] \quad ;$$

$$\mathrm{k}^2 = (c/\omega)^2 (k^2 + k_y^2) \quad . \tag{10}$$

In this paper the mechanical surface impedance of the panel is stated in the simple but orthotropic form

$$Z_p(k, \omega_2) = i\omega m [1 - \{(k/k_p)^2 + (k_y/k_{py})^2\}^p] , \tag{11}$$

where m is the mass per unit area and $\{k_p, k_{py}\}$ is the free wavevector on the panel. The panel is membrane-like if p = 1, and is plate-like responding in flexure if p = 2. The free orthotropic wavevector $\underline{k}_p$ is written in the form

$$\underline{k}_p = \{k_p, k_{py}\} ; \quad k_p = k_{po} (1 - i\eta_p) ; \quad k_{py} = k_{pyo}(1 - i\eta_{py}) ;. \quad \underline{k}_{po} = \{k_{po}, k_{pyo}\} \quad , \tag{12}$$

where $\{\eta_p, \eta_{py}\}$ is the loss factor "vector". For a plate and a membrane that is made to simulate a plate responding in flexure

5

$$k_{po}^2 = (\omega\omega_c \, / \, c^2); \qquad k_{pyo}^2 = (\omega\omega_{cy} \, / \, c^2) \, ; \quad |k_{po}| = (k_{po}^2 + k_{pyo}^2)^{1/2} \, , \qquad (13)$$

where ω_c and ω_{cy} are the critical frequencies in the x- and y-domain, respectively. These critical frequencies are defined with respect to the speed of sound c in the fluid facing the panel. For a plate in longitudinal response and a membrane in flexural response

$$k_{po}^2 = (\omega \, / \, \omega_c)^2 \, (k_c)^2 \, (c \, / \, c_{\ell})^2; \qquad k_{pyo}^2 = (\omega \, / \, \omega_{cy})^2 \, (k_{cy})^2 \, (c \, / \, c_{\ell y})^2, \qquad (14)$$

where $\{k_c, k_{cy}\} = \{(\omega_c \, / \, c), (\omega_{cy} \, / \, c)\}$ and the free wave velocity in the panel is $\{c_{\ell}, c_{\ell y}\}$. The surface admittance may then be derived from Eqs. (8), (9), and (11) in the explicit form

$$G_{\infty} \, (k, \omega_2) = [Z_{\infty} \, (k, \omega_2)]^{-1};$$
$$Z_{\infty} \, (k, \omega_2) = (i \, \omega \, m) \, [1 - \{(k \, / \, k_p)^2 + (k_y \, / \, k_{py})^2\}^P - (i \, \varepsilon_c) \, (k_3 c / \omega_c)^{-1}] \, , \qquad (15)$$

where the fluid loading parameter ε_c is defined

$$\varepsilon_c = (\rho \, c \, / \, \omega_c m) \, . \qquad (16)$$

In this paper the panel is assumed to be isotropic; $k_{po} = k_{pyo}$; $\eta_p = \eta_{py}$, $\omega_c = \omega_{cy}$. The orthotropic form for the mechanical surface impedance of the panel is stated to indicate that simple orthotropy can be readily accommodated in the estimations of the response.

The line impedance and line moment impedance of a typical rib may be cast in various forms some of which may be elaborated to reflect the various properties that the ribs and their attachment to the panel may possess [1]. In this paper the explicit expressions for the line impedance and line moment impedance are cast in the simple forms

$$Z_j = Z = i \, \omega \, (M_g + M_o) \, ; \qquad M_o = M \, \{1 - (\omega \, / \, \omega_o)^2 \, (1 - i \, \eta_o)\}^{-1} \, , \qquad (17)$$

6

$$Z_{Mj} = Z_M = i\,\omega\,(M / k_{Mo}) \quad ; \quad k_{Mo} = k_M \left\{ 1 - (\omega / \omega_{Mo})^2 (1 - i\,\eta_{Mo}) \right\} (M / M_o),$$

$$(18)$$

respectively, where M_g and M are masses per unit length, k_M is a specified wavenumber, ω_o and ω_{Mo} are given resonance frequencies, and η_o and η_{Mo} are assigned loss factors. The line impedance of the rib, stated in Eq. (17), is slightly more elaborate than that assumed in Reference 2 in that a mass controlled impedance ($i\omega M_g$) is added and placed adjacent to the panel [1]. Also, the line moment impedance of a typical rib is included here.

From Eqs. (4), (15), (17), and (18) one obtains

$$\tilde{H}_{\infty}(k, \omega_2) = \left[(M_g/mb) + (M_o/mb)\{ 1 - i(k / k_{Mo})\} \right]$$

$$\left[1 - \left\{ (k / k_p)^2 + (k_y / k_{py})^2 \right\}^P - i\,\varepsilon_c\,(k_3 c/\omega_c)^{-1} \right] .$$

$$(19)$$

Again, the elaborations introduced in Eqs. (17) and (18) and, in turn, in Eq. (19), are not employed directly in this paper; they are included in order to indicate the readiness with which they can be accommodated in the estimations.

ESTIMATIONS OF THE RESPONSE OF AND THE PRESSURE ABOVE THE PANEL

Uniform environmental loadings and fluid loading in particular, can be readily accommodated in the computations; i.e., there is no difficulty inserting Eqs. (4) and (8) in general, and Eqs. (15) and (19) in particular, in Eq. (6). The resulting equation evaluates the response of the panel merely in terms of summations over harmonics with respect to the separation wavenumber κ_1; $\kappa_1 = (2\pi/b)$. For reasonable panels, ribs, and fluid loading, the summations can be approximated by a small number of terms, therefore the computations can be handled by a desk top computer. [cf. Appendix A.]

The pressure spectral distribution $P(k, \omega_2, z)$ in the fluid on a plane a distance z above the panel is derived directly from the velocity spectral distribution $V(k, \omega_2)$ on the surface of the panel; namely,

$$P(k, \omega_2, z) = \exp(-i k_3 z) Z_f(k, \omega_2) V(k, \omega_2), \qquad (20)$$

where

$$Z_f(k, \omega_2) = Z_{tf}(k, \omega_2) = (\rho\omega / k_3) = \rho c (k_3 c/\omega)^{-1}, \qquad (21)$$

and use is made of Eq. (9) [1]. The explicit expression for $(k_3 c/\omega)$ is given in Eq. (10). Thus, once the velocity spectral distribution of the panel is estimated, the pressure spectral distribution on a plane a distance z above the panel readily follows, as stated in Eq. (20), where $Z_f(k, \omega_2)$ represents the conversion factor from the spectral distribution of the velocity $V(k, \omega_2)$ of the panel to the spectral distribution of the pressure $P(k, \omega_2, 0)$ [$\equiv P(k, \omega_2)$] in the fluid on the surface of the panel. With this interpretation, the factor $\exp(-i k_3 z)$ represents the filtering performed by propagation through the slab of fluid between the surface of the panel and a control plane above it where the pressure is estimated [1]. Eq. (10) shows that, for a supersonic component in $P(k, \omega_2)$, this filtering is a mere phase change — propagation without decay. For a subsonic component in $P(k, \omega_2)$, this filtering is an exponential decay with an exponent that increases linearly with the normal distance of the control plane above the panel.

NORMALIZATIONS AND DISPLAYS

The preceding formalism is used to calculate the spectral distributions of the response of several representative cases of interest. The response quantities chosen are the acceleration $A(k, \omega_2)$ on the surface of the plate [which is simply related to the velocity $V(k, \omega_2)$ and/or displacement $D(k, \omega_2)$; see Eq. (1)] and the pressure $P(k, \omega_2, z)$ in the fluid on a control plane placed a normal distance z above the surface of the plate. The relevant spectral distributions are cast in the normalized forms:

8

$$\overline{A}(k, \omega_2) = A(k, \omega_2)\,[P_{ea}(\omega_2)/m]^{-1} = (\omega/\omega_c)\,\overline{V}(k, \omega_2)\ ;$$

$$\overline{V}(k, \omega_2) = V(k, \omega_2)\,[P_{ca}(\omega_2)/i\omega_c m]^{-1}\ , \tag{22}$$

$$\overline{P}(k, \omega_2, z) = P(k, \omega_2, z)\,[P_{ea}(\omega_2)\,(\varepsilon_c/i)]^{-1}\ , \tag{23}$$

where ε_c is defined in Eq. (16). Only magnitudes of these quantities are displayed. By and large, these magnitudes are displayed clipped by certain predetermined and convenient clipping values (thresholds) so that only magnitudes that exceed these thresholds are shown. The clipping values are designated by a superscript of zero; e.g., the clipping values of $|\overline{A}|$ and $|\overline{P}|$ are thus designated $|\overline{A}^{\,o}|$ and $|\overline{P}^{\,o}|$, respectively [2]. The estimations may be conveniently displayed on planes defined by any two of the normalized dependent variables (k/κ_1), (k_y/κ_1), and (ω/ω_c), with the third held fixed. In this paper, the $\{(k/\kappa_1), (\omega/\omega_c)\}$-plane is used and the magnitudes of a quantity are computed as a function of the normalized wavenumber (k/κ_1), at specific, equal, and successive values of the normalized frequency (ω/ω_c) with a fixed value of (k_y/κ_1) [2]. Also, the computations are focused on limited portions of the $\{(k/\kappa_1), (\omega/\omega_c)\}$-plane; usually the lower wavenumber and frequency portions. [The graphs are displayed in the format of Figs. 3 and 4 of Reference 2; acquaintance with the format of these figures will assist readers unacquainted with these display procedures.]

COMPUTER ESTIMATIONS

In Section II, the parameters of influence on the estimated magnitudes of interest are:
p, (c_ℓ/c), (k_y/κ_1), (M/mb), η_p, (bk_c), (ω_o/ω_c), η_o, (bk_M), (ω_{Mo}/ω_c), η_{Mo}, (ω_c/ω_{cy}), $(c_\ell/c_{\ell y})$, (η_p/η_{py}), (zb), (x_a/b), ε_c, $|\overline{A}^{\,o}|$, $|\overline{P}^{\,o}|$, etc. In describing the figures, it is convenient to define a set of standard conditions for the estimations of the spectral distributions of the magnitudes of the response. The standard conditions are:

The panel is isotropic,

$$(M/mb) = 0.3, \ (bk_m) = 10^6, \ (bk_c) = 16, \ (bk_y) = 0 \quad , \quad (x_a/b) = 0.3 \quad ;$$

$$|\overline{A}^o| = 1.4, \ |\overline{P}^o| = 1.4, \ \text{and}$$

$$\eta_p = \begin{cases} 5 \times 10^{-3} & , \ p = 1 \\ 2.5 \times 10^{-3} & , \ p = 2 \end{cases} \quad ; \quad \varepsilon_c = \begin{cases} 0.1 \ \text{with fluid loading} \\ 0.0 \ \text{with fluid loading removed} \end{cases} \quad . \tag{24}$$

Note that the standard conditions are defined with the thresholds $|\overline{A}^o|$ and $|\overline{P}^o|$ equal. The standard conditions are conveniently defined so that only departures need reporting in the text and figure captions. Figure 2 displays a set of computed estimates relating to the acceleration spectral distribution of line driven unribbed panels. In Fig. 2a the acceleration spectral distribution on an unribbed fluid loaded membrane is displayed; the membrane is made to simulate the dispersion properties of a plate responding in flexure. [cf. Fig. 4 of Reference 2.] The expected vanishing of the response of the panel at the sonic loci and the associated sonic gorge is clearly discernable. In Fig. 2b the corresponding estimations for an unribbed fluid loaded plate responding in flexure are displayed. The analogies and differences between the response on a membrane that simulates a plate in flexure and a plate in flexure can be deciphered by comparing Fig. 2a with Fig. 2b. Except for minor details, the patterns in the response show that a membrane can be analytically modeled to simulate the response of a plate in flexure. [cf. Eqs. (13) and (14).] The clipped version of Fig. 2b is displayed in Fig. 2c.

The corresponding pressure spectral distributions on a plate responding in flexure and on a plane some distance above it are shown in Figs. 3a and b, respectively. The manner in which the acceleration spectral distribution converts into the pressure spectral distribution on the surface of the panel is illustrated by comparing Figs. 2b and 3a; the absence of the sonic gorge in the spectral distribution of the pressure is noted. Indeed, not only is the sonic gorge ironed out but moderate peaks occur at the sonic loci and a sonic ridge is formed. The suppression of subsonic

10

components in the pressure spectral distribution on a plane parallel to the panel as the plane is further removed from the panel is illustrated by comparing Figs. 3a and b [cf. Eqs. (10) and (20)].

The computed estimations relating to the response of a regularly ribbed panel that is mostly fluid loaded and mostly plate-like is now introduced. The displays are in the format of Fig. 2c in that the magnitudes displayed are clipped. In Appendix A, the formalism stated in Eq. (6) admits readily to accounting for fluid loading and/or to accounting for regularly ribbed plates responding in flexure. It is intended just to illustrate the influence of fluid loading on panels that are plates responding in flexure; other kinds of panels (e.g., membranes) and other types of reponses (e.g., longitudinal) which were widely used in Reference 2, are omitted for brevity.

Figure 4 displays the clipped magnitudes of the acceleration of a regularly ribbed fluid loaded plate responding in flexure. In this figure the line impedance of each of the identical ribs is assumed to be mass controlled, and the line moment impedance is assun   to be negligible. The clipping value in all of Fig. 4 is identical. The acceleration spectral distribution of a standard fluid loaded, regularly ribbed and isotropic plate; i.e., $(M/mb) = 0.3$, $\eta_p = 2.5 \times 10^{-3}$, $(bk_c) = 16$, $\omega_c = \omega_{cy}$, $\eta_p = \eta_{py}$, and $\varepsilon_c = 0.1$, is depicted in Fig. 4a. Figure 4b is the same as Fig. 4a except that fluid loading is removed by setting $\varepsilon_c = 0$. [In this connection, it is noted that a fluid loading represented by $\varepsilon_c = 0.1$ is "heavy".] The similarities between the displays shown in Fig. 4a and b are clear enough. However, close observation shows minor dissimilarities; e.g., the dispersion peaks occur at slightly different loci in Fig. 4a and b. A fairly common procedure replaces fluid loading on a panel by adding surface mass and increasing the loss factor to compensate for the radiation damping. How adequate is such a procedure? The computation performed may be used to answer this question in part. A surface mass of (p/k_{p1}) is added to the surface mass of the panel and the distributed damping designated by η_p is increased by the factor γ, where k_{p1} is the free wavenumber on the panel corrected for fluid loading and $\gamma > 1$. To accommodate this procedure, fluid loading is ignored and the mechanical surface impedance of the isotropic panel is replaced instead by

11

$$Z_p(k, \omega_2) = i\omega m \left[1 + (\rho/mk_{p1}) - \{(k^2 + k_y^2)/k_p^2\}^P \right] \quad ;$$

$$k_p = k_{po}(1 - i\gamma\eta_p) \quad ; \quad k_p^2 = (\omega\omega_c/c^2) \quad , \tag{25}$$

where

$$1 + (\rho/mk_{p1}) = (k_{p1}/k_{po})^{2P} \quad . \tag{26}$$

[cf. Eqs. (11) and (15).] If one finds that k_{p1} can be approximated by k_{po} in Eq. (26) then in Eq. (25) one may set

$$(\rho/mk_{p1}) = (\rho/mk_{po}) = (\omega_c/\omega)^{1/2} \varepsilon_c \quad . \tag{27}$$

Figure. 4c illustrates the use of this procedure for the standard (moderate) conditions under which Fig. 4a is obtained. The similarities between Figs. 4a and c are increased and the dissimilarities are decreased as compared to those between Figs. 4a and b; e.g., the dispersion peaks are substantially coincident in Figs. 4a and c. However, closer examination, especially in the unclipped versions of these figures, shows that the sonic gorge is not present in Fig. 4c. At and in the vicinity of the sonic region, the similarities between Figs. 4b and c are closer than those between Figs. 4a and c. This indicates that the above procedure for accounting for fluid loading may, with caution, be useful for certain purposes.

In Fig. 5 the mass ratio (M/mb) is increased from 0.3 to the rather large value of 3: otherwise the standard conditions imposed on Fig. 4a remain intact. In Fig. 5a the fluid loading remains standard at $\varepsilon_c = 0.1$. In Fig. 5b the fluid loading is removed; $\varepsilon_c = 0$. Comparing Figs. 5a and b reveals that fluid loading does significantly influence the patterns when the line impedance of a typical rib is "heavy." This kind of influence of fluid loading supports the notion that fluid loading tends to "mend and soften" the discontinuities associated with attaching heavy ribs to the panel [3-5].

12

In Fig. 6 the line impedance of a typical rib is decreased and the line moment impedance of a typical rib is introduced. This is accomplished by choosing a mass ratio of $(M/mb) = 0.05$ and $(k_M b) = 9$. [In Figs. 4 and 5 the line moment impedance of a typical rib is removed by setting $(k_M b) = 10^6$; see Eq. (24).] In Fig. 6 the line moment impedance is mass controlled as is the line impedance. In Fig. 5a fluid loading is present with $\varepsilon_c = 0.1$, and in Fig. 5b fluid loading is removed by setting $\varepsilon_c = 0$. The similarities and dissimilarities between Figs. 6a and b are analogous to those found between Figs. 4a and b. The introduction of line moment impedances shows no dramatic effects in the response of the panel to a line drive.

Attention is now focused on computer estimations of the pressure spectral distribution on and above the plane of the regularly ribbed fluid loaded panel. [cf. Figs. 3a and b.] Figs. 7a, b, and c display the magnitudes of the pressure spectral distribution above a plate responding in flexure and under standard conditions; see Eq. (24). In Fig. 7a the pressure spectral distribution is that on the surface of the plate; $(zk_c) = 0$. In Figs. 7b and c the magnitudes of the pressure spectral distribution are those on control planes removed by $(zk_c) = 2$ and by $(zk_c) = 12$, respectively, normally off the plate. The suppression of the subsonic components by this removal is clearly evident, as is the sonic ridge. Comparing Figs. 3a and b and Fig. 7 illustrates the contribution that ribs make to the pressure spectral distribution. The contribution made by the ribs in the supersonic region is of particular interest. In this connection, comparing Figs. 4a and 7a again reveals the depression at and in the vicinity of the sonic region in Fig. 4a, and the enhancement at and in the vicinity of the corresponding spectral region in Fig. 7a. Indeed, a sonic gorge in Fig. 4a is the counterpart to a sonic ridge in Fig. 7; e.g., Fig. 7b [6].[1] The dominant influence of fluid loading

---

[1] One needs to differentiate between the spectral distribution of the pressure in a plane above the surface of a vibrating surface and the pressure radiated to a localized spatial region above the surface. These two manifestations of the pressure field are related but not coincident. Indeed, characteristics exhibited in one may not be exhibited in the other. Stretching a point to illustrate the statement, consider a panel vibrating under a local external drive. The sonic ridge will be present in the spectral distribution of the pressure on a plane removed somewhat from the panel. [cf. Figure 2e.] On the other hand, the pressure radiated to a localized region on that plane, but that is far removed from the location of the external drive will not track the sonic ridge, notwithstanding

at and near the vicinity of the sonic range is thus manifested; the influence is dominant because the fluid surface impedance in that spectral range is the dominant term in the surface impedance of the panel. Again, these displays, and those presented in Reference 2 were given to briefly establish the kind, the type, and the wide range of computer estimations that can be conducted in terms of the formalism presented. No attempt was made to cover a specific feature of interest. This coverage can be provided when a specific question or need arises.

---

that the contribution to this radiated pressure, at grazing angles, is contributed by the near sonic components on the plane of the panel. The lack of tracking is explained when one realizes that the radiated pressure is contributed by the appropriate spectral components on the plane of the panel that are related to the velocity and not to the pressure. The far field radiated pressure tracks, by and large, the spectral distribution of the velocity and not of the pressure [6].

APPENDIX A

COMMENTS ON IRREGULAR RIBBING

It is crucial to realize that the simplicity in the computations afforded in Eq. (6) is in direct consequence of the regularity of the ribs and their attachment to the panel. For irregularly ribbed panels this simplicity is not afforded. If the panel is not regularly ribbed, it becomes necessary to evaluate the (transfer) line admittance [1]

$$g_\infty (x, \omega_2) = (2\pi)^{-1/2} \int G_\infty (k, \omega_2)\, dk \exp (-ikx) \quad .$$

(A1a)

Moreover, when the panel can support a moment response, it becomes necessary to evaluate also the derivative of $g_\infty (x, \omega_2)$ with respect to x; namely [1]

$$g'_\infty (x, \omega_2) = (\partial/\partial x)\, g_\infty (x, \omega_2) \quad .$$

(A1b)

In the absence of fluid loading the integration involved in Eq. (A1) is simple enough, but is difficult when fluid loading is included [3-5]. Moreover, since the response of the ribbed panel is a functional of $g_\infty (x, \omega_2)$, and, when appropriate also of $g'_\infty (x, \omega_2)$, and these functions must be evaluated over an extensive number of values of x which are not simply related, the evaluation of the response is beset by difficulties that are compounded. This is the sense in which Eq. (6) is considered relatively simple. The regularity replaces the integral, and, when appropriate, its derivative with respect to x, by evaluations at a number of discrete values of the wavenumber. Indeed, one may claim that the regularity in the rib spacing not only facilitates accounting for the fluid loading but also for determining the response of a plate in flexure. In the case of a plate

15

responding in flexure, the integral in Eq. (A1) is more complicated than it is for a mere membrane. Finally, the regularity of the separations among the ribs is more significant than the identity of the line impedances and, when appropriate, also the identity of the line moment impedances of the ribs. The discrete values in the wavenumber, which are introduced by the harmonics with respect to κ_1, are not destroyed by relaxing the identity of the line and line moment impedances of the ribs [2]. Thus, it is conceivable that one could relax the requirement for the identity of the impedances of the ribs without entirely forfeiting the advantages that an equation like Eq. (6) holds in accounting for the fluid loading and, when appropriate, in accounting also for "the plate in flexure" properties of the panel.
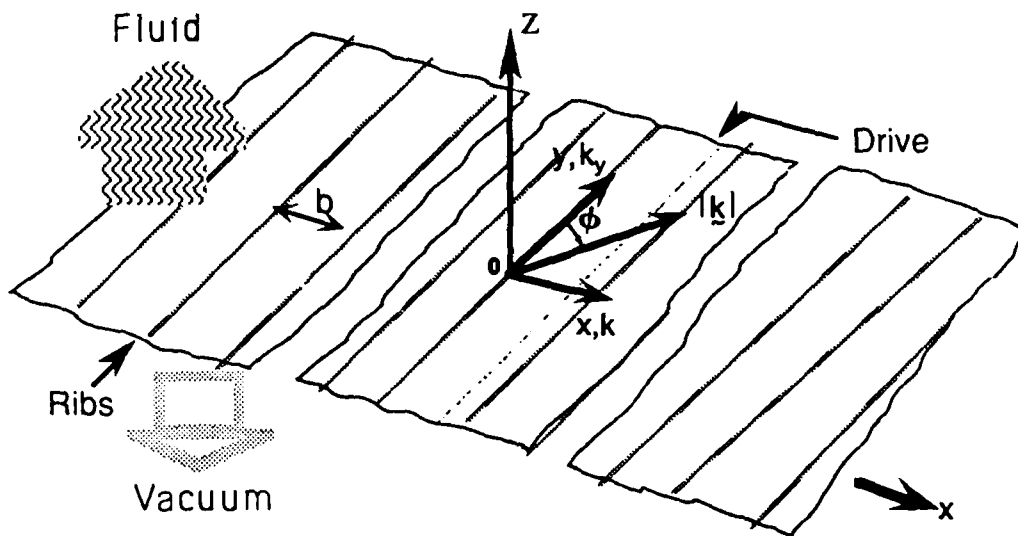
Fig. 1. A sketch of a regularly ribbed fluid loaded panel showing the coordinate system and the orientation and locations of the ribs and the external line drive.
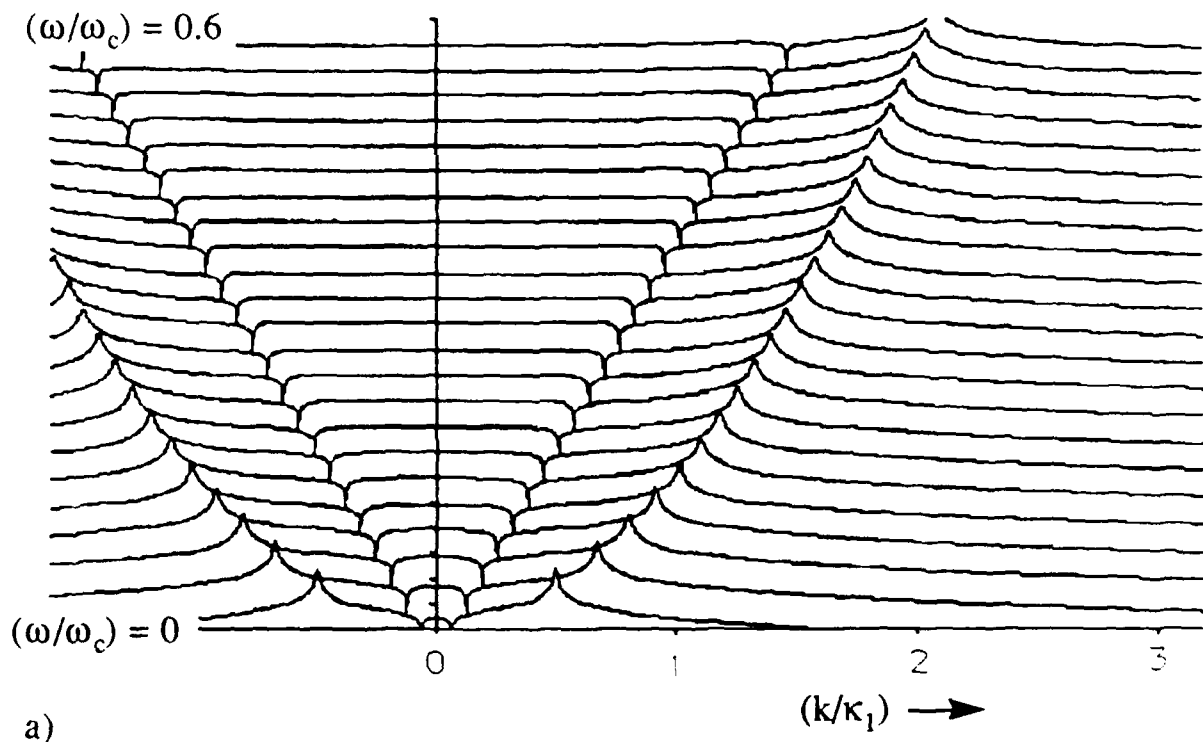

a)

Fig. 2. Magnitudes of the acceleration spectral distribution for an unribbed fluid loaded panel under standard conditions [Eq. (24)] as a function of the normalized wavenumber (k/κ_1) at successive and equal increments of the normalized frequency (ω/ω_c).
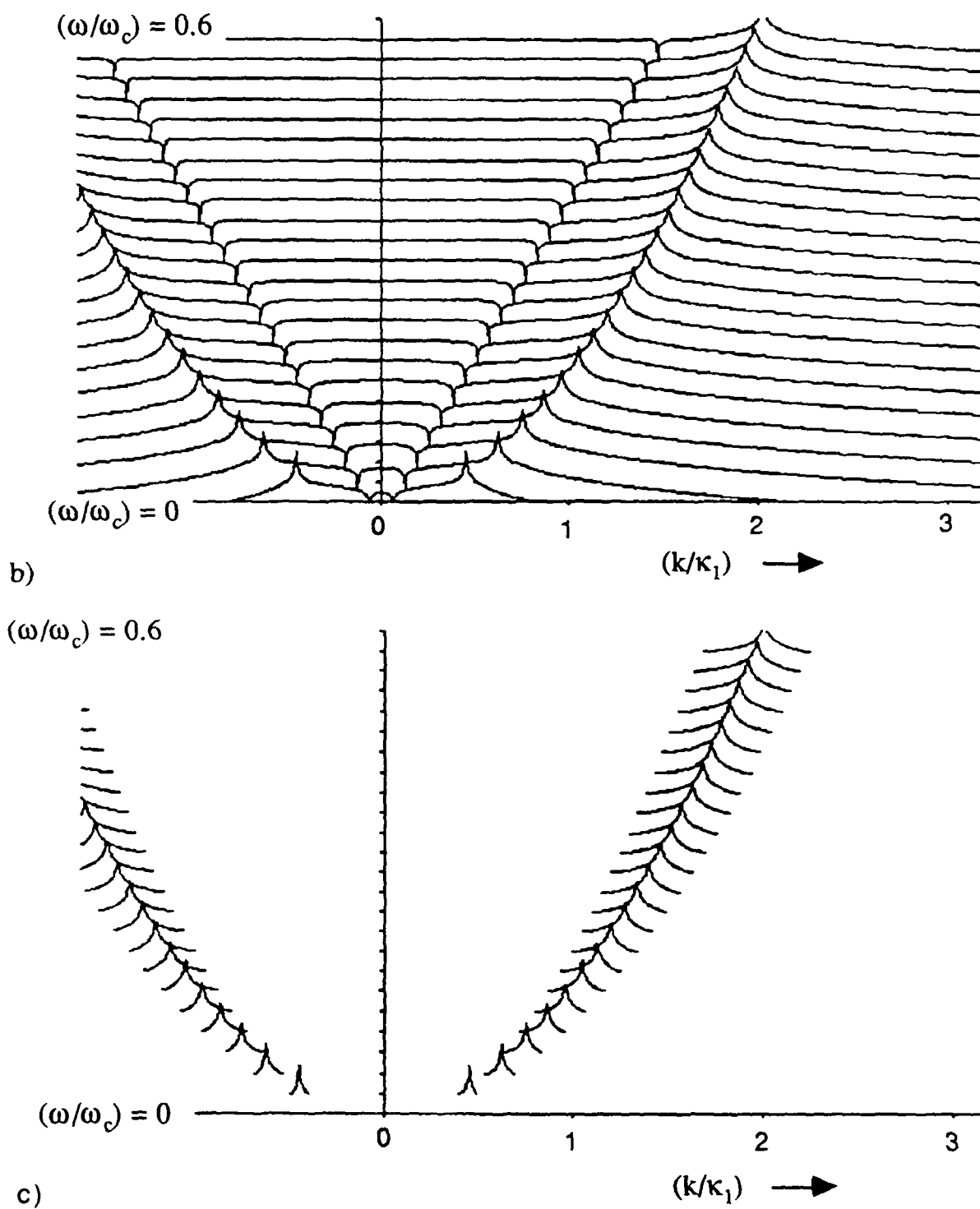
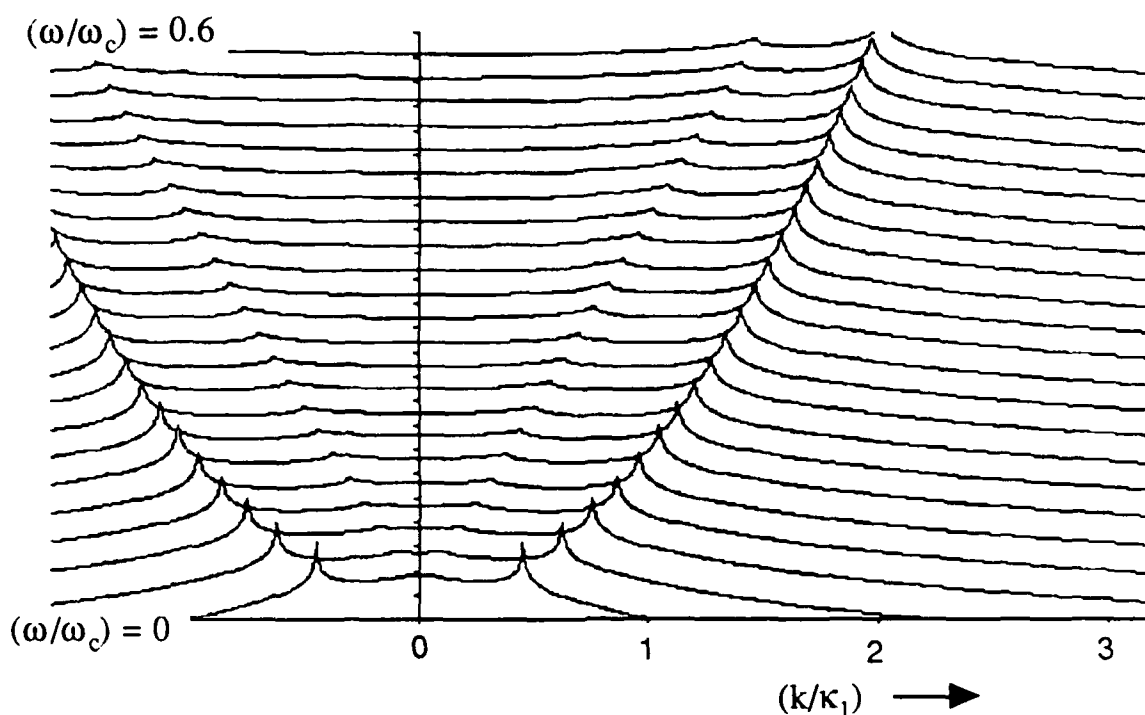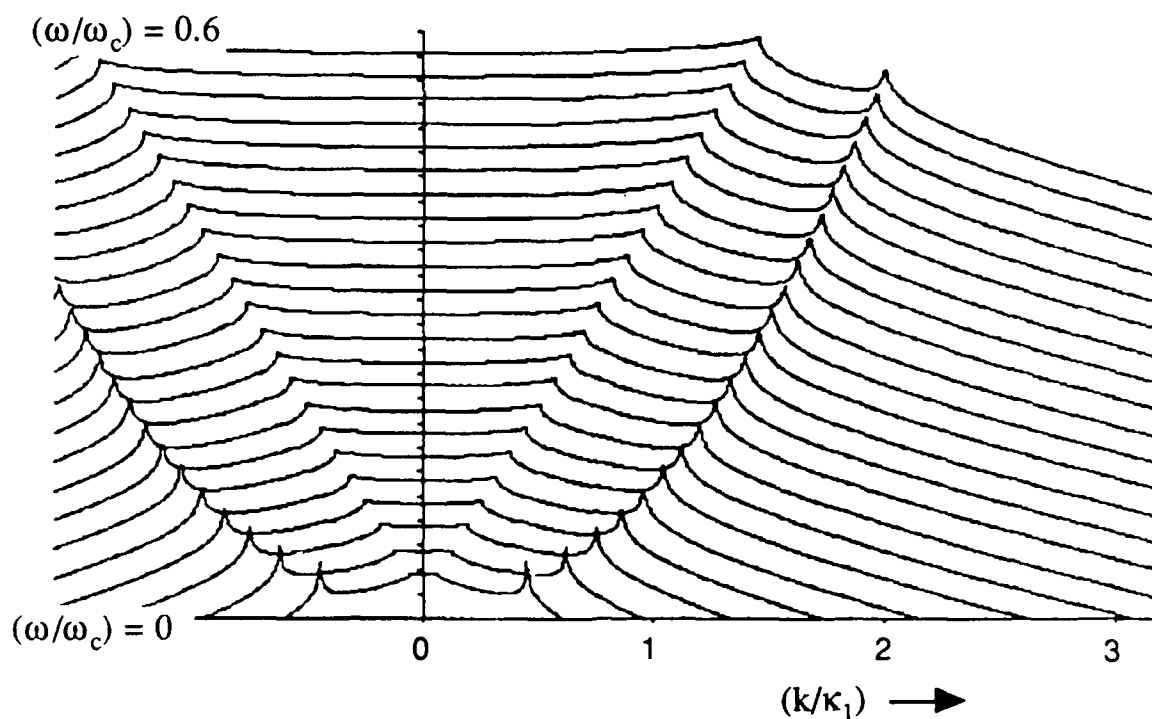a. A membrane that simulates a plate; $p = 1$.

17

b)

c)

Fig. 2 (continued)
(b) A plate in flexure; p = 2.
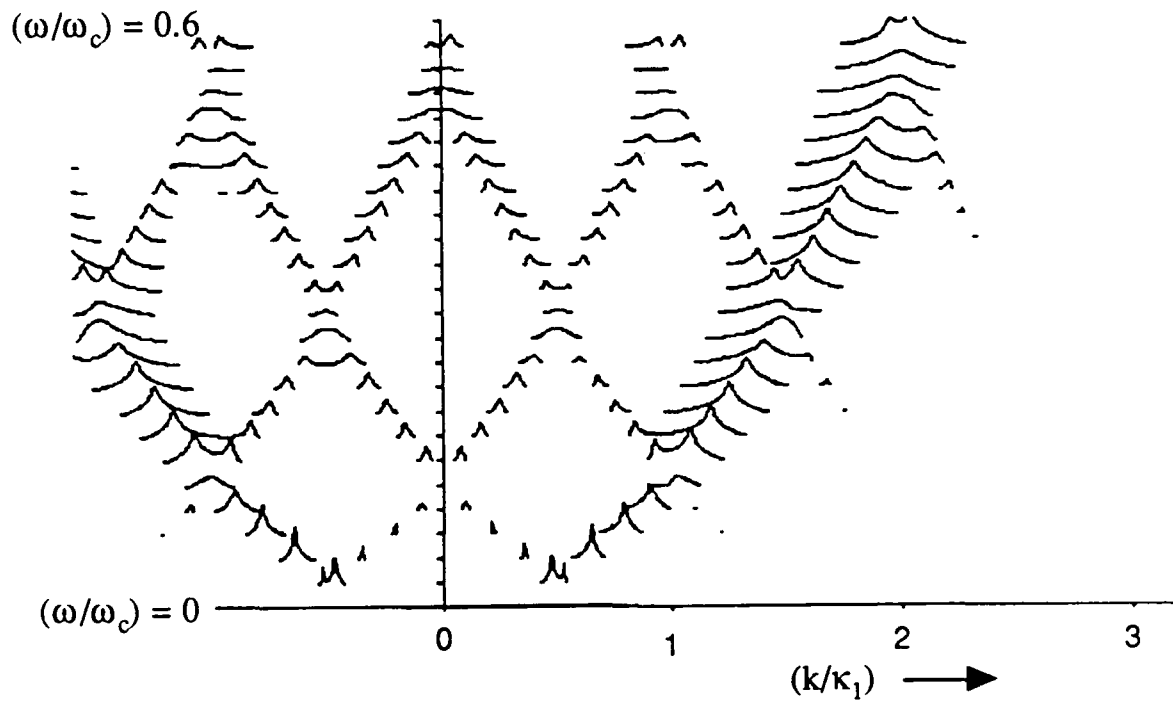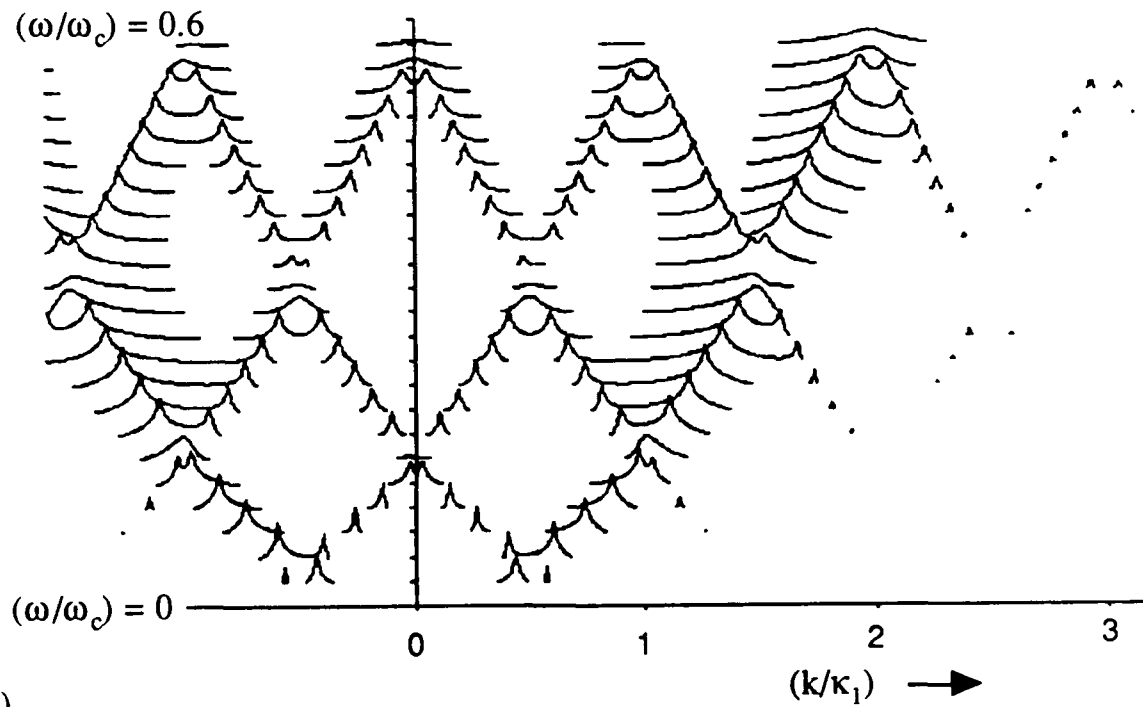(c) A clipped version of Fig. 2b.

a)

b)

Fig. 3. Magnitudes of the pressure spectral distribution on a plane above
an unribbed fluid loaded plate under standard conditions [Eq. (24)] as a
function of the normalized wavenumber (k/κ_1) at successive and equal
increments of the normalized frequency (ω/ω_c).

(a) $(k_c) = 0$.

(b) $(zk_c) = 12$.

19

$(\omega/\omega_c) = 0.6$

$(\omega/\omega_c) = 0$

(k/κ_1) ⟶

a)

$(\omega/\omega_c) = 0.6$

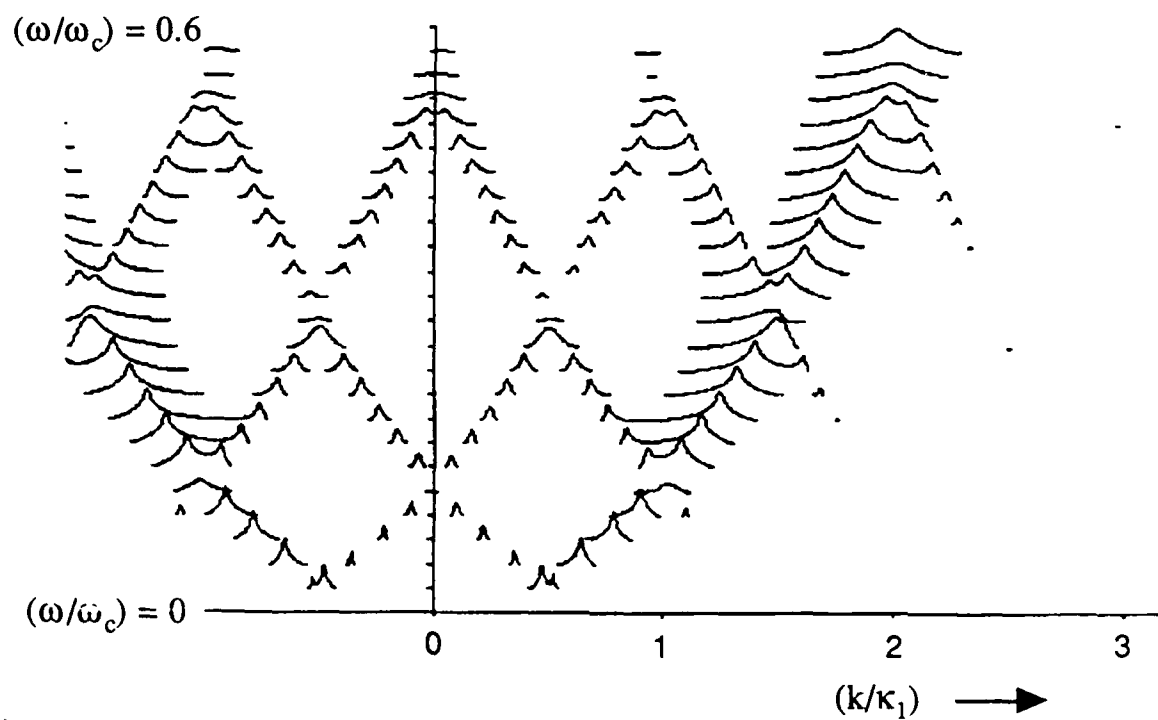$(\omega/\omega_c) = 0$

(k/κ_1) ⟶

b)

Fig. 4. Magnitudes of the acceleration spectral distribution of a regularly ribbed plate responding in flexure under standard conditions [Eq. (24)] as a function of the normalized wavenumber (k/κ_1) at successive and equal increments of the normalized frequency (ω/ω_c).

(a) $\varepsilon_c = 0.1$.

(b) $\varepsilon_c = 0.0$.

20

$(\omega/\omega_c) = 0.6$

$(\omega/\bar{\omega}_c) = 0$

$(k/\kappa_1) \longrightarrow$

c)

Fig. 4 (continued)
(c) Introduction of fluid loading in the manner specified in Eqs. (25)
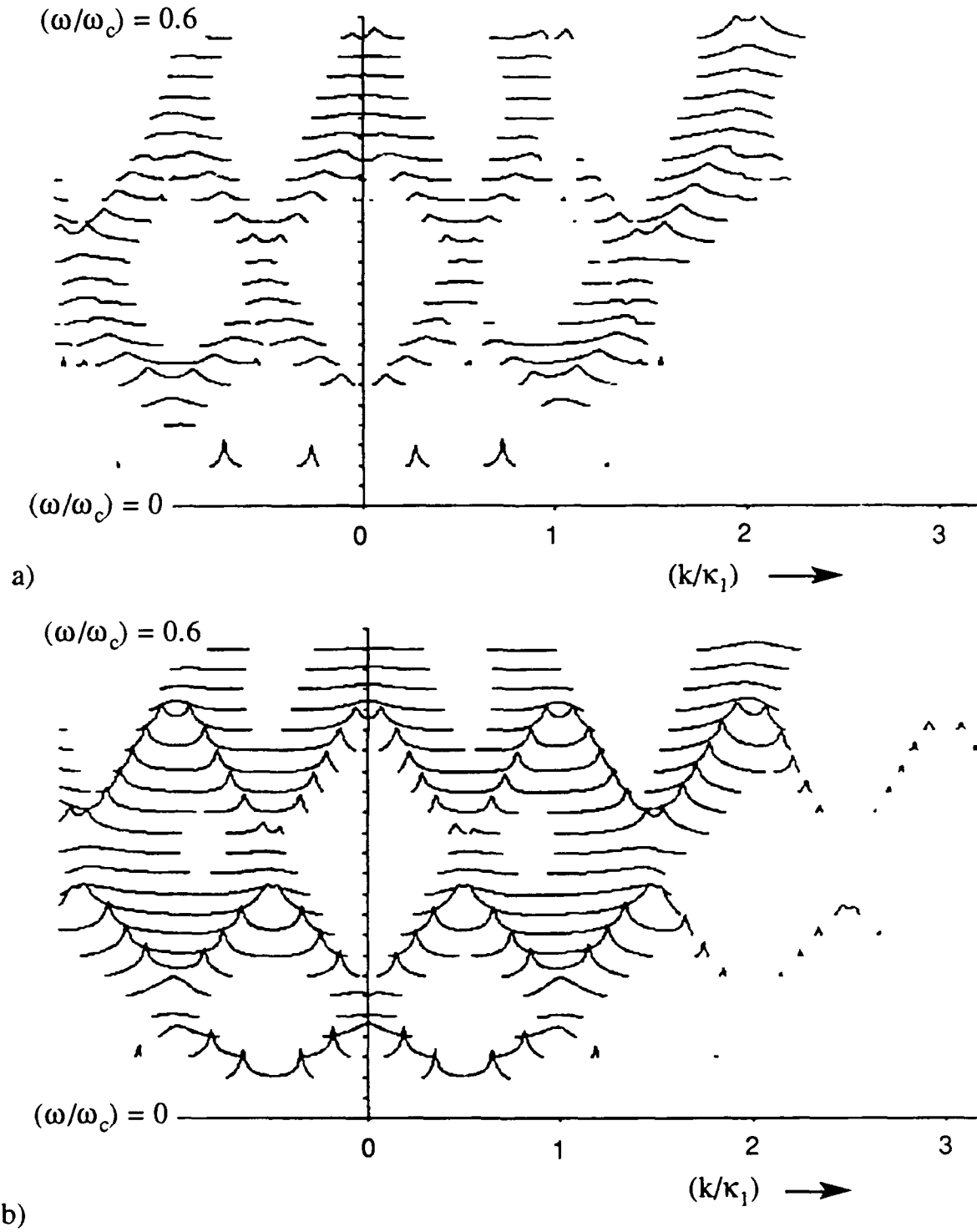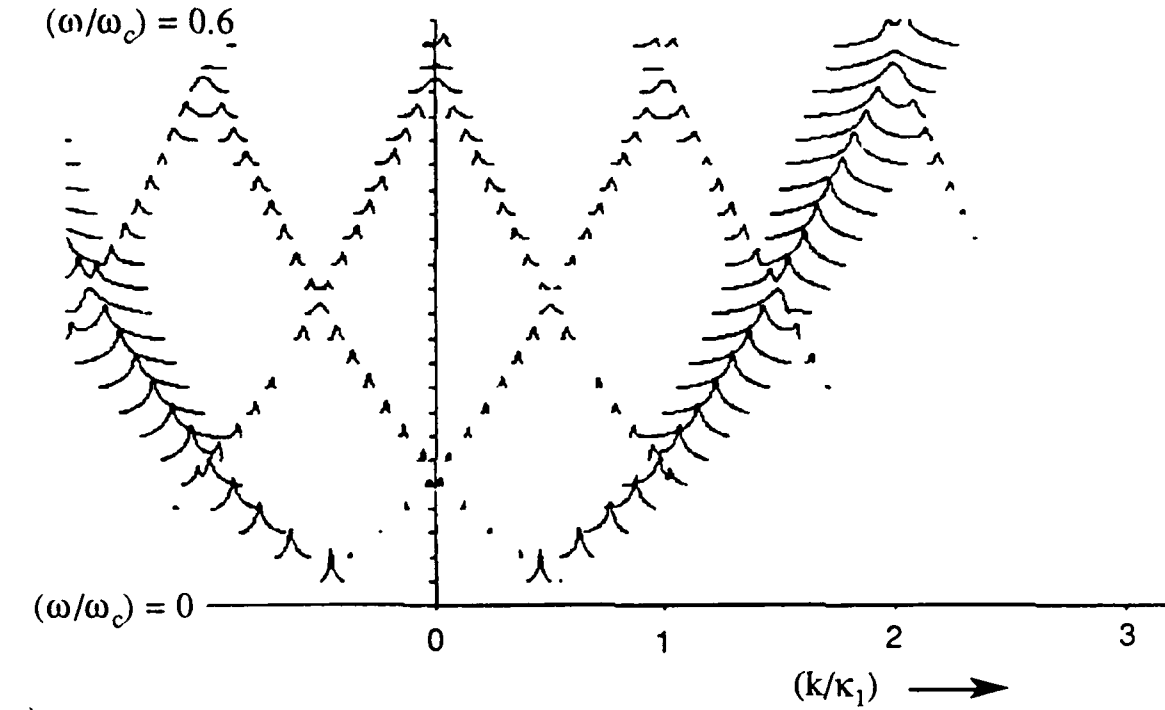through (27) with $\varepsilon_c = 0.1$ and $\gamma = 2$.

$(\omega/\omega_c) = 0.6$

$(\omega/\omega_c) = 0$

(k/κ_1) ⟶

a)

$(\omega/\omega_c) = 0.6$
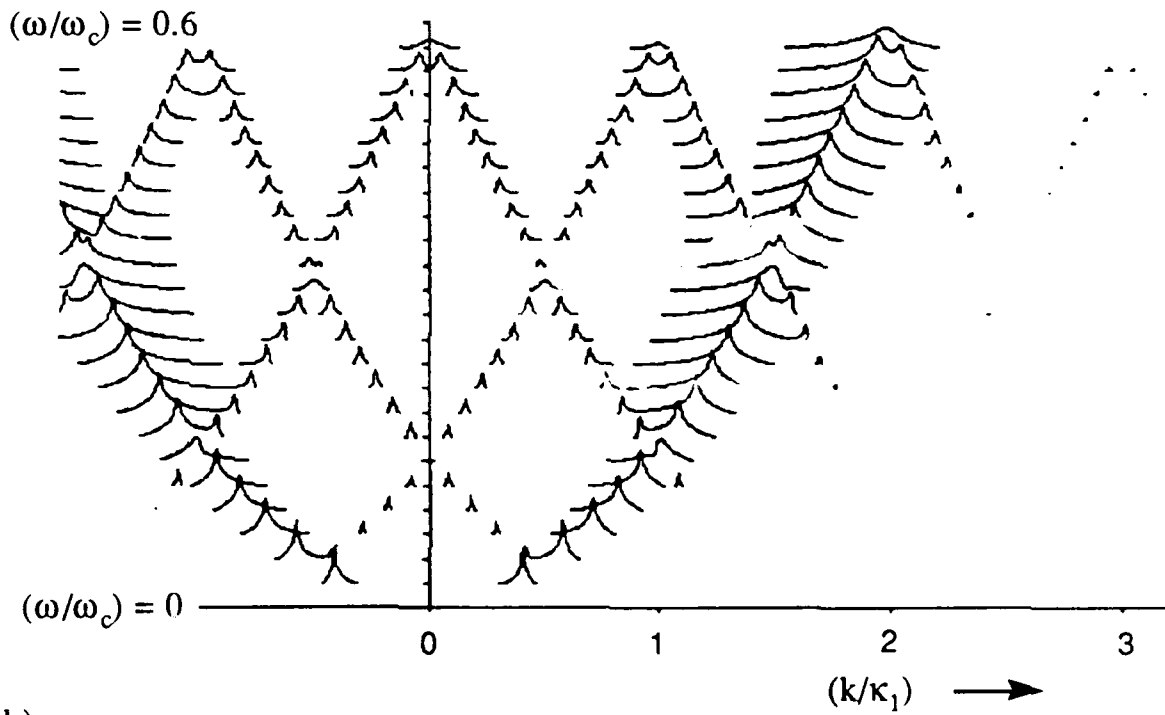
$(\omega/\omega_c) = 0$

(k/κ_1) ⟶

b)

Fig. 5. As in Fig. 4 except that the mass ratio (M/mb) is increased from the standard value of 0.3 to 3.
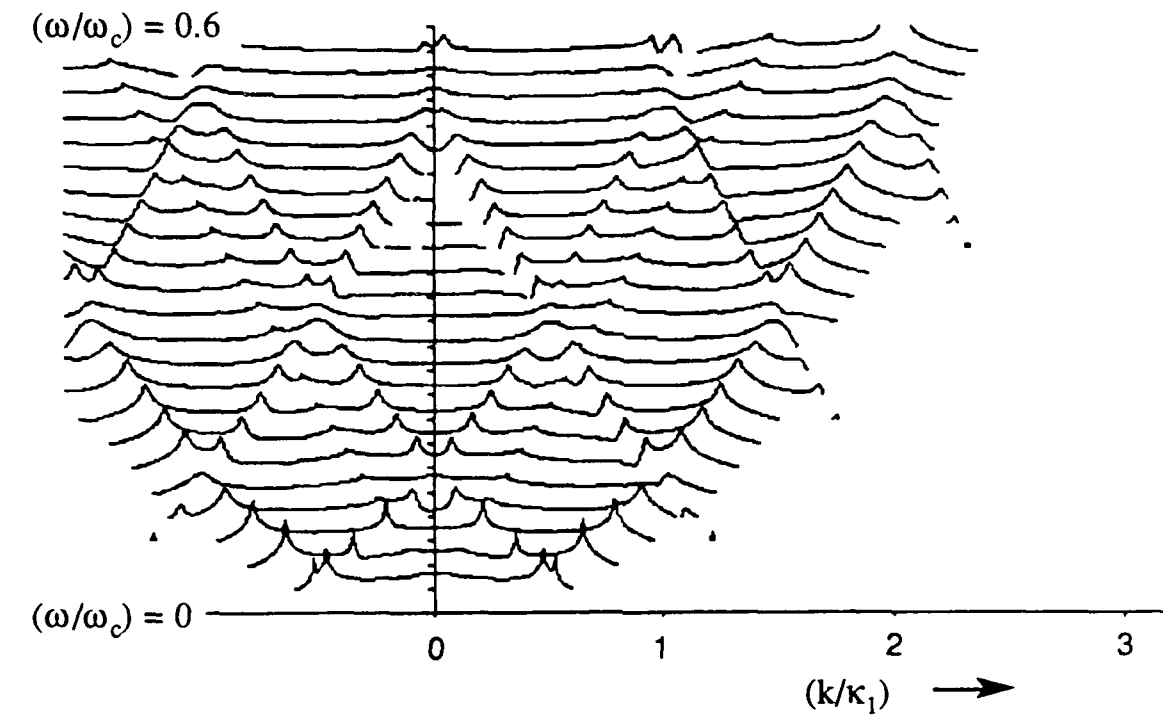
(a) $\varepsilon_c = 0.1$.
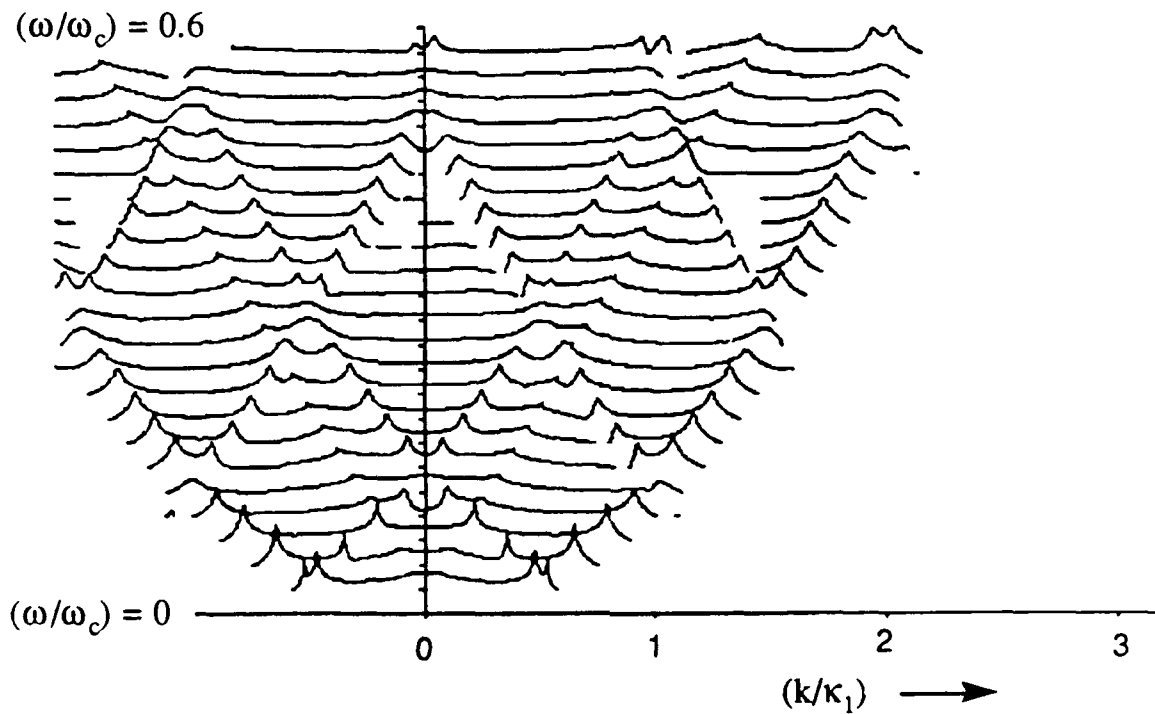(b) $\varepsilon_c = 0.0$.

Fig. 6. As in Fig. 4 except that the mass ratio (M/mb) and the normalized moment wavenumber (bk_M) are decreased from their standard values of 0.3 and 10^6, respectively, to the values of 0.05 and 9, respectively.
(a) $\varepsilon_c = 0.1$.
(b) $\varepsilon_c = 0.0$.

23

$(\omega/\omega_c) = 0.6$

$(\omega/\omega_c) = 0$

$(k/\kappa_1) \longrightarrow$

a)

$(\omega/\omega_c) = 0.6$

$(\omega/\omega_c) = 0$

$(k/\kappa_1) \longrightarrow$

b)

Fig. 7. Magnitudes of the pressure spectral distribution on planes above the surface of a regularly ribbed fluid loaded plate responding in flexure under the standard conditions [Eq. (24)], as functions of the normalized wavenumber (k/κ_1) at successive and equal increments of the normalized frequency (ω/ω_c). [cf.Fig. 3.]

(a) $zk_c = 0$.

(b) $zk_c = 2$.

24

$(\omega/\omega_c) = 0.6$

$(\omega/\omega_c) = 0$

(k/κ_1) ⟶

0   1   2   3
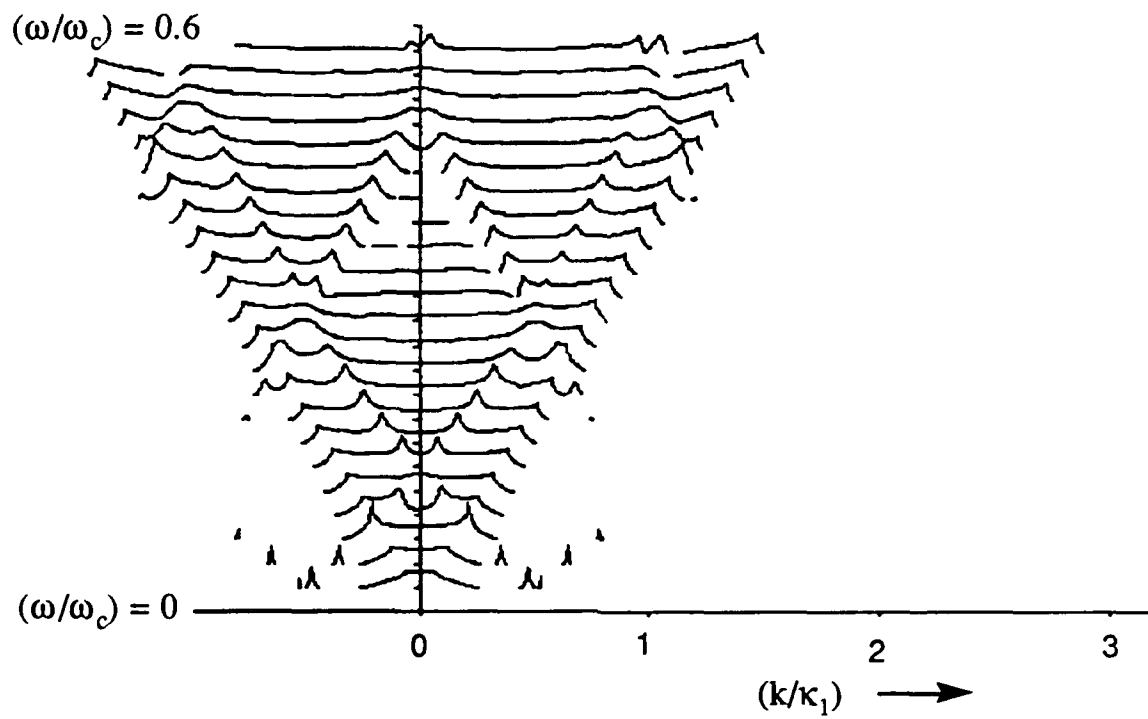
c)

Fig. 7. (continued)
(c) $(zk_c) = 12$.

REFERENCES

1. Maidanik, G. and J. Dickey, 1988, *Journal of Sound and Vibration* , 123, 293 - 307. Acoustic behavior of ribbed panels.

2. Maidanik, G. and J. Dickey, 1989, *Journal of Sound and Vibration* , 000, 000-000. Velocity distribution on unloaded finitely and regularly ribbed membranes.

3. Nayak, P. R., 1970, *Journal of the Acoustical Society of America*, 47, 191-201. Line admittance of infinite isotropic fluid-loaded plate.

4. Maidanik, G., A. J. Tucker and W. H. Vogel, 1976, *Journal of Sound and Vibration*, 49 (4), 445-452. Transmission of Free waves across a rib on a panel.

5. Crighton, D. G., 1980, *Journal of Sound and Vibration*, 68, 15-33. Approximation to the admittances and free wavenumbers of fluid-loaded panels.

6. Maidanik, G., J. Dickey and J. Ertel, 1989, *Journal of Sound and Vibration*, 000, 000-000 Partial radiation efficiency of line driven panels.

INITIAL DISTRIBUTION

Copies			Copies		
2	ONT (Remmers)		1	1905.3 (Feit)	
3	ONR		1	1906 (Vendettis)	
	121 (Hansen)		1	1908 (McKeon)	
	11 (Reischmann)		1	192	
	1132SM (Abraham)		1	1921 (King)	
3	NAVSEA		1	1926 (Keech)	
	2 SEA 55N (Biancardi)		1	193	
	1 SEA 92R		1	194	
1	DARPA		1	1941 (Kilcullen)	
12	DTIC		1	1944 (Maga)	
5	USNA Physics Depart. (Ertel) Stop 25				
			1	27	
CENTER DISTRIBUTION			1	2704	
1	01A		10	2704.1	
1	0112 (Halsall)		1	274	
1	0113		1	2741	
			1	2742	
1	17		1	2743	
1	172		1	2744	
			1	2749	
1	18				
			1	284	
1	19				
1	1902		1	342.1	TIC(C)
1	1903 (Smith)		1	342.2	TIC(A)
1	1905.1 (Blake)		2	3431	
			10	3432	Reports Control

REPORT DOCUMENTATION PAGE

Public reporting burden for this collection of information is estimated to average 1 hour per response, including the time for reviewing instructions, searching existing data sources, gathering and maintaining the data needed, and completing and reviewing the collection of information. Send comments regarding this burden estimate or any other aspect of this collection of information, including suggestions for reducing this burden, to Washington Headquarters Services, Directorate for Information Operations and Reports, 1215 Jefferson Davis Highway, Suite 1204, Arlington, VA 22202-4302, and to the Office of Management and Budget, Paperwork Reduction Project (0704-0188), Washington, DC 20503.

1. AGENCY USE ONLY (Leave blank)	2. REPORT DATE November 1990	3. REPORT TYPE AND DATES COVERED

4. TITLE AND SUBTITLE
Response of Regularly Ribbed Fluid Loaded Panels

5. FUNDING NUMBERS

6. AUTHOR(S)
G. Maidanik and J. Dickey

7. PERFORMING ORGANIZATION NAME(S) AND ADDRESS(ES)
David Taylor Research Center
Annapolis, MD 21402
Code 27

8. PERFORMING ORGANIZATION REPORT NUMBER
DTRC–90/036

9. SPONSORING /MONITORING AGENCY NAME(S) AND ADDRESS(ES)
David Taylor Research Center
Annapolis, MD 21402
Code 27

10. SPONSORING /MONITORING AGENCY REPORT NUMBER

11. SUPPLEMENTARY NOTES

12a. DISTRIBUTION /AVAILABILITY STATEMENT
Approved for public release, distribution is unlimited.

12b. DISTRIBUTION CODE

13. ABSTRACT (Maximum 200 words)
This paper presents computer estimations of the response of models of mechanically driven regularly ribbed fluid loaded panels. The estimates are presented in terms of the spectral distribution of the acceleration of the panel and the spectral distribution of the pressure in the fluid. The ribs are defined in terms of line and line moment impedances; these may be mass, resistance, and/or stiffness controlled, and of various values and combinations. Typical estimations of the spectral distribution of the magnitudes of the acceleration are displayed as functions of the normalized wavenumber that lies in the plane of the panel and normal to the ribs and the normalized frequency. The magnitudes of the acceleration vanish at the sonic loci when fluid loading is included. A sonic gorge, with a nadir at the sonic loci, characterizes the acceleration of the fluid loaded panel, whether unribbed or ribbed. If the magnitudes of the line impedances (and, when appropriate, also the line moment impedances) of the ribs are not unusually high, the magnitudes of the acceleration and their patterns elsewhere in the spectral domain remain substantially similar to those obtained in the absence of fluid loading. The dissimilarities are readily accounted for by straightforward arguments relating to the increase in the surface mass and the radiation damping that manifest fluid loading on panels. The corresponding magnitudes of the pressure on the surface of the panel do not vanish at the sonic loci and a sonic ridge replaces the sonic gorge. The loss of subsonic components in the pressure on a plane, as the plane is removed from the surface of the panel, is clearly displayed.

14. SUBJECT TERMS
Fluid loaded panels; Sonic peak

15. NUMBER OF PAGES
28

16. PRICE CODE

17. SECURITY CLASSIFICATION OF REPORT Unclassified	18. SECURITY CLASSIFICATION OF THIS PAGE Unclassified	19. SECURITY CLASSIFICATION OF ABSTRACT Unclassified	20. LIMITATION OF ABSTRACT